

# UDV methods for characterizing flows in liquid metal batteries

Jonathan Cheng<sup>1</sup>, Bitong Wang<sup>1</sup>, Ibrahim Mohammad<sup>1</sup>, Gerrit Horstmann<sup>2</sup>, Douglas Kelley<sup>1</sup>

<sup>1</sup>Dep. of Mechanical Engineering, University of Rochester, Rochester, NY 14627, USA

<sup>2</sup>Dep. of Helmholtz-Zentrum Dresden-Rossendorf, Dresden 01328, Germany

We present ultrasound measurements from a laboratory model of a liquid metal battery (LMB). Two major flow drivers interact within LMBs: thermal gradients due to the presence of internal heating, and electrovortex flow (EVF) driven by diverging current densities. The product of these interactions remains poorly characterized. We approach this problem with ultrasonic Doppler velocimetry (UDV) combined with a laboratory model of an LMB fluid layer. Using ultrasound probes placed around a liquid gallium vessel, we elucidate typical velocities, flow structures, and flow statistics in a representative volume of the flow field. UDV measurements reveal that pure convection takes the form of the recently-discovered ‘jump rope vortex,’ with a characteristic frequency visible in velocity statistics. They also indicate that EVF goes through stable, unstable, and oscillatory flow regimes. In progress is an approach for training physics-informed neural networks (PINNs) on UDV data, allowing us to reconstruct flow in regions where no probe measurements have taken place by leveraging the equations of motion.

**Keywords:** Industrial flow, Velocimetry, Liquid metals, Convection, Magnetohydrodynamics

## 1. Introduction

Over the course of a day, energy demand in the US can vary by up to 50% in a given region [1]. For renewable sources like wind and solar power, energy production cannot be dynamically controlled and instead subject to the whims of the environment. This means that a time lag often exists between the hours of peak production and peak demand, requiring rapid ramping of nonrenewable energy supplies which lead to operational inefficiencies and, in the case of a large renewable presence, potential waste of surplus energy. Grid-scale energy storage is one way to curb these inefficiencies. Among the variety of storage technologies in development, liquid metal batteries (LMBs) stand out as being particularly cost-effective [2]. Much of this owes to the liquid nature of the battery: construction becomes simpler, damage to the reactive components is self-healed, and materials are inexpensive.

However, the fluid nature of LMBs lends them a strong propensity for flow: a variety of thermal, chemical, and electromagnetic forces play against one another in both helpful and harmful ways [3,4]. The fluid dynamics occurring in LMBs can be paramount to their operation. Leading approaches to understanding LMB flows generally center on direct numerical simulations [5,6]. However, laboratory experiments provide some distinct advantages: we can efficiently conduct surveys over broad ranges of the governing parameters. By varying two or more forcing factors in the flow, we can construct phase diagrams that indicate when transitions in flow morphology take place. Laboratory setups also allow us to verify whether the physics in idealized simulations actually manifest the same way in real-world settings.

To make laboratory measurements relevant to LMBs, opaque liquid metals must be employed. This greatly limits which velocity measurement techniques are useful; most particle tracking, Schlieren, and dye based techniques become unviable. Ultrasonic Doppler

Velocimetry (UDV) is perhaps the best option available under these circumstances. Instead of measuring a 2D flow field, UDV only measures along 1D lines, meaning that special care must be taken in the planning stages to ensure that it succeeds in characterizing the flow field.

In this study, we discuss a variety of methodologies for making UDV measurements within a layer of liquid gallium under thermal and electromagnetic flow forcings. UDV uncovers myriad and interesting flows occurring in a laboratory model of a liquid metal battery. In section 2 we discuss the theoretical background for LMB flows. In section 3, we describe the fundamentals of UDV and the experimental design considerations for optimizing our UDV measurements. In section 4, we show results and elaborate on our postprocessing methods for UDV data.

## 2. Theoretical background

Figure 1a is a schematic of a liquid metal battery. LMBs are identical in principle to solid batteries: they are galvanic cells with two materials – the cathode and anode – which undergo an energetically favorable reaction. These are separated by a third material in the middle, an electrolyte which allows positive ions through and forces electrons to find an alternate pathway. They are a developing technology, with various container geometries and chemical compositions currently being explored [2]. It is thus important to develop a broad understanding of how different flow forcings interact with one another via scaling laws between governing parameters that can be generalized to different systems.

Two of the most prominent drivers of flow are thermal gradients and electromagnetic forces. A thermal gradient which leads to lighter fluid above denser fluid is stabilizing. In the reverse case, unstable thermal gradients lead to convection, characterized by the Rayleigh number:

$$Ra = \frac{\alpha g \Delta T H^3}{\nu \kappa} \quad (1)$$

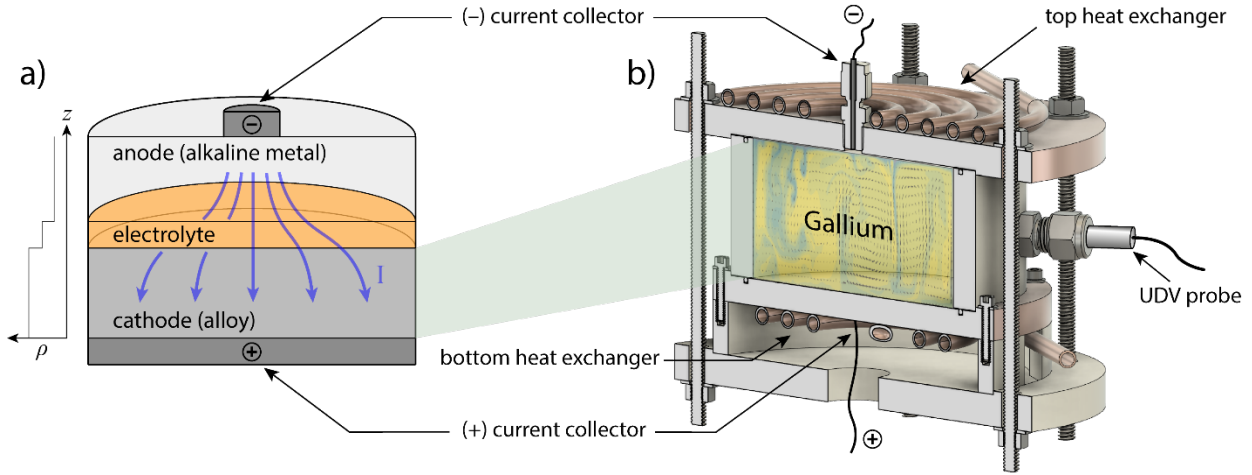


Figure 1: Schematic demonstrating how our novel experimental setup models a layer of a liquid metal battery. Panel a) shows that liquid metal batteries are composed of three fluid layers, each with greater density than the layer above it. The top current collector is typically narrower than the bottom leading to a horizontally diverging current density. Panel b) is a design drawing of our laboratory setup. The top current collector is a narrow copper cylinder while the bottom is the copper plate forming the bottom boundary of the gallium fluid layer. The sidewall of the container is made of nonconductive acetal plastic. UDV probes are placed in the sidewalls and top lid of the setup. The flow field visualized in the container is from simulations by Personnetaz *et al.* [6].

where  $\alpha$  is the coefficient of thermal expansion,  $g$  is gravitational acceleration,  $\Delta T$  is the magnitude of the temperature gradient,  $H$  is the height of the container,  $\nu$  is kinematic diffusivity, and  $\kappa$  is the thermal diffusivity.

While many forms of electromagnetic flow could occur in LMBs, we focus on one prominent player known as electrovortex flow (EVF). EVF is induced by horizontally diverging current densities. The strength of EVF is characterized by a so-called EVF parameter [7,8]:

$$S = \frac{\mu_0 I^2}{4\pi^2 \rho \nu^2} \quad (2)$$

where  $\mu_0$  is the vacuum permeability,  $I$  is the imposed current, and  $\rho$  is the fluid density.

Our apparatus is designed to explore the combination of convection or stable stratification with EVF. One way to quantify the resultant flows with an overall descriptor of system dynamics, the Reynolds number  $Re = UD/\nu$  where  $L$  is a typical length scale and  $U$  is a typical flow speed.

### 3. Experimental design

#### 3.1 Ultrasonic Doppler Velocimetry

We use Signal Processing transducers to perform our UDV measurements. Velocities are measured along a straight line in front of each probe. Ultrasonic pulses are released in quick succession from the probe and backscattered by particles in the fluid. Velocities as a function of time are determined by the shift in position of these particles between pulses: particles moving toward the probe register a negative velocity while those moving away from the probe have positive velocity. Probes operate at 4 MHz or 8 MHz. Rather than seeding particles in the fluid, naturally occurring oxide particles serve as the scattering agent in our study. Up to 9 ultrasound probes are placed in various locations around the container.

#### 3.2 Apparatus

Figure 1b shows a design drawing of our device. The working fluid is liquid gallium, which is liquid near room temperature, confined to a cylindrical space of diameter  $D = 10$  cm and height  $H = 5$  cm (Aspect ratio  $\Gamma = 2$ ). The top and bottom boundaries are copper plates. To each plate is soldered a copper coil which serves as a heat exchanger: two thermal baths recirculate water through

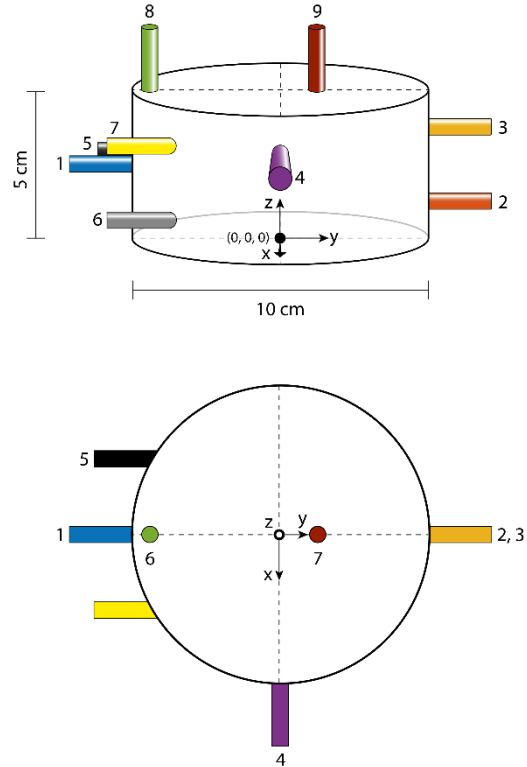


Figure 2: Distribution of UDV probes around the gallium fluid layer. They are positioned to optimally capture expected flow structures in convection and EVF.

each of these coils such that either a stabilizing or destabilizing temperature gradient can be imposed on the gallium layer. The spirals are wound non-inductively to prevent horizontal temperature gradients. The sidewall of the vessel is a 1.1cm thick Delrin cylinder, a non-conductive material that ensures all currents pass through the gallium layer.

Currents from 0 to 90 Amperes are controlled by a power supply. The negative electrode is a copper rod of diameter 1/4 in attached to the top plate. It is separated from the top copper plate by a plastic fitting such that current lines do not pass through the plate. The bottom plate is mated to a copper rod connected to the power supply: with the high conductivity of copper, the entire bottom plate forms the positive electrode. With a diameter ratio between electrodes of  $\Gamma_e = 0.06$ , a large horizontal divergence in the current lines trigger EVF. Figure 2 shows the locations of UDV probes throughout the system. Positions are limited by the shape of our vessel: each probe requires clearance while the electrode and copper coils on the top plate also occupy space.

Literature predicts that convection and EVF take the form of overturning rolls in the tank. In the former case, flow rises along the centerline and falls along the sidewalls [9] while in the latter, a vertical jet descends along the centerline inducing rising flow along the sidewalls [8]. We therefore place two vertical probes facing down into the fluid layer: one near the center line and one close to the sidewall. Strong horizontal flows should be situated near the top and bottom of the tank, with a transition from positive to negative velocities near the middle. Thus, horizontal radial probes are situated at  $z = 0.75H$  and  $z = 0.25H$  (and at different angles to account for non-axisymmetric behaviors). Three probes oriented along chord positions ( $x = -0.25D, 0.25D$ ) at different heights are used to detect azimuthal flows, which are known to arise in EVF when external magnetic fields are involved.

## 4. Results

### 4.1 UDV data

Figure 3a shows a typical Dopplergram from a convection case, absent any imposed current. Instead of a steady flow, an obvious periodic behavior dominates the flow: this can be seen in both the time-dependent, spatially averaged data (Figure 3c) and the fast Fourier transform (FFT) spectrum (Figure 3d). The peak frequency corresponds to a recently-discovered mode known as the ‘jump rope vortex,’ where the core of the overturning circulation orbits around a horizontal axis [10]. This mode may encourage greater mixing than previously expected in LMBs.

Figure 4 shows several Dopplergrams from EVF cases over a range of  $S$  values. Here, the flow clearly undergoes a behavioral transition from stable in Figure 4a to unstable in Figure 4c. In the intermediate range, Figure 4b, a curious transition occurs involving periodic behaviors. Such clear periodicity has not been previously observed in this transition to our knowledge, and further study is warranted.

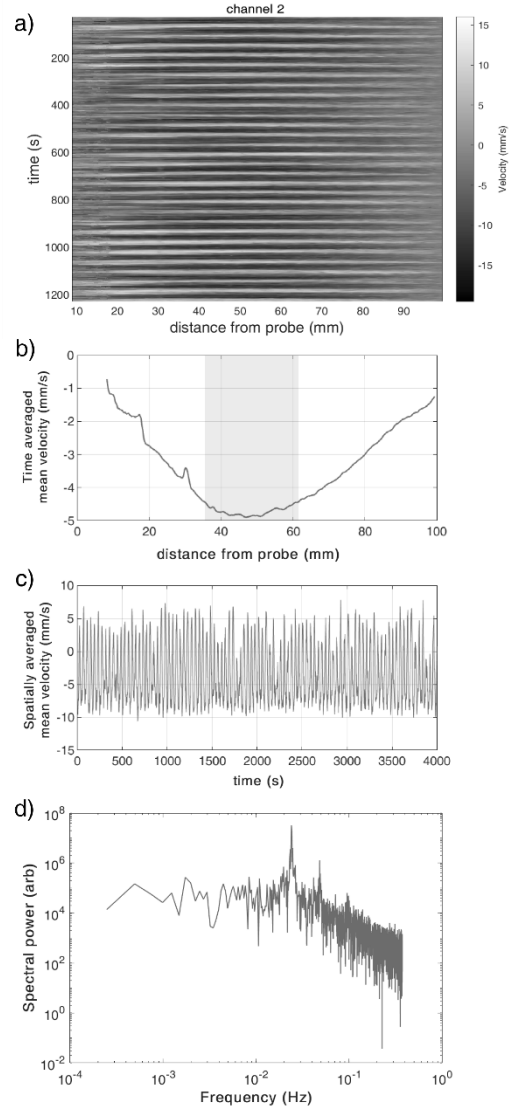


Figure 3: UDV data from convection at  $Ra = 2.04 \times 10^5$ . Panel a) shows a Dopplergram for probe 2 (see Figure 2): time plotted versus distance from probe with color representing velocity. Panel b) shows the time-averaged velocity versus distance from probe and panel c) the spatially averaged mean velocity versus time. Panel d) shows that the periodic signature visible in a) and c) corresponds to a prominent frequency peak at 0.024 Hz.

### 4.2 Analysis and postprocessing

Translating UDV results to characteristic velocities and flow structures is nontrivial. Since probes are only positioned in select locations and only detect the component of flow parallel to them, we must ascertain which portion of a UDV Dopplergram – both spatially and temporally – represent characteristic velocities.

In Figure 5, we use several different methods to estimate the Reynolds number from raw UDV data, comparing the resultant  $Re$  vs.  $Ra$  scaling laws against those in the literature. The caption contains more details on these methods. Although absolute  $Re$  values vary, each method still delivers very similar best-fit scalings. They also agree closely with theoretical scaling laws from Ahlers *et al.* [11], who predict  $Re \propto Ra^{0.4}$  for these parameter ranges.

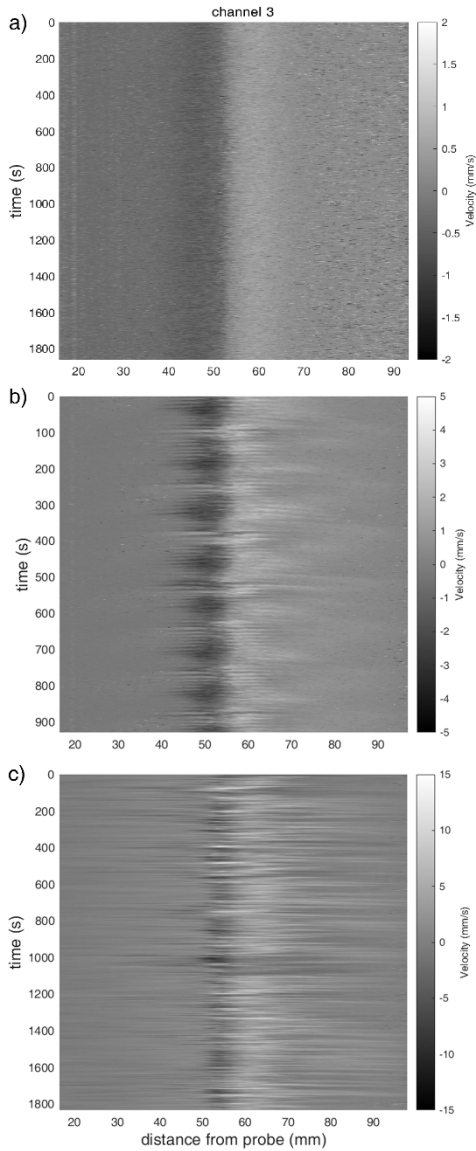


Figure 4: UDV Dopplergrams of probe 3 (see Figure 2) in electrovortex flow cases, at a)  $S = 1.05 \times 10^3$ , b)  $S = 9.47 \times 10^3$ , c)  $S = 6.74 \times 10^4$ . As  $S$  increases the flow transitions from stable to periodic to unstable.

Large spatial data gaps are inevitable with UDV. We are exploring the viability of using Physics-Informed Neural Network (PINN) to fill in these data gaps in a reliable way. PINNs are a machine learning tool that takes into account not only the input data but also how well results match the governing equations of motion. This allows the neural network to make an educated guess at the morphology and velocity of flow between different probe lines.

## 5. Summary

In this work we have shown that UDV is an effective technique for determining the flows occurring in LMBs, eventually helping to predict how flows will affect batteries in an industrial setting. Convective signals manifest a periodic signature of the recently discovered jump-rope vortex, and velocity estimates from UDV show strong agreement with previous studies and theoretical

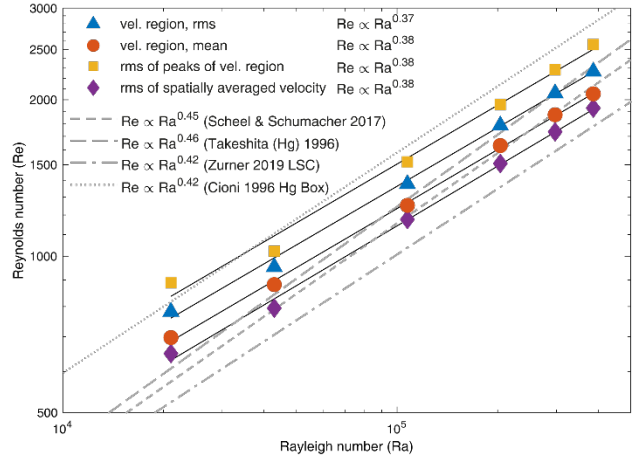


Figure 5:  $Re$  vs.  $Ra$  data plotted for several different methods of estimating typical velocities from UDV data. Triangles, circles, and squares only take into account the ‘velocity region,’ where the flow is likely parallel to the UDV probe direction (see highlighted region in Figure 3b). Triangles use the root mean square velocity over all time, circles take the mean over all time, and squares only consider times when the velocity magnitude is near its peak. Finally, diamonds consider the velocities over the region. Data between all probes are averaged in each case. Previous measurements from the literature are plotted in gray.

predictions. EVF undergoes behavioral transitions as the imposed current is varied, showing stable and unstable regimes with periodic behaviors at the transition. PINNs are a promising, if nascent, approach to filling in the necessarily large spatial gaps characteristic of UDV data.

## References

- [1] <https://www.eia.gov/todayinenergy/detail.php?id=42915>
- [2] Kim H, *et al.*: Liquid metal batteries: past, present, and future, *Chem. Rev.* 113.3 (2013), 2075-2099.
- [3] Kelley DH, & Weier T: Fluid mechanics of liquid metal batteries, *App. Mech. Rev.* 70.2 (2018).
- [4] Weber N, *et al.*: Electromagnetically driven convection suitable for mass transfer enhancement in liquid metal batteries, *Appl. Therm. Eng.* 143 (2018), 293-301.
- [5] Shen Y & Zikanov O: Thermal convection in a liquid metal battery, *Theor. Comput. Fluid Dyn.* 30.4 (2016), 275-294.
- [6] Personnetaz P, *et al.*: Mass transport induced asymmetry in charge/discharge behavior of liquid metal batteries, *Electrochem. Comm.* 105 (2019), 106496.
- [7] Lundquist S: Hydromagnetic viscous flow generated by a diverging electric current, *Ark. Fys.* 40 (1969), 89-95.
- [8] Davidson PA: *An Introduction to Magnetohydrodynamics*, Cambridge University Press, Cambridge (2002).
- [9] Ashour RF, *et al.*: Competing forces in liquid metal electrodes and batteries, *J. of Power Sources* 378 (2018), 301-310.
- [10] Vogt T, *et al.*: Jump rope vortex in liquid metal convection, *Proc. Natl. Acad. Sci.*, 115.50 (2018), 12674-12679.
- [11] Ahlers G, *et al.*: Heat transfer and large scale dynamics in turbulent Rayleigh-Bénard convection, *Rev. Mod. Phys.* 81.2 (2009), 503.